

Metamagnetic transition and reversible magnetocaloric effect in antiferromagnetic DyNiGa compound

Yan-Hong Ding(丁燕红), Fan-Zhen Meng(孟凡振), Li-Chen Wang(王利晨), Ruo-Shui Liu(刘若水), Jun Shen(沈俊)

Citation: Chin. Phys. B . 2020, 29(7): 077501 . **doi:** 10.1088/1674-1056/ab90f3
Journal homepage: http://cpb.iphy.ac.cn; http://iopscience.iop.org/cpb

What follows is a list of articles you may be interested in

Magnetic properties of the double perovskite compound Sr_2YRuO_6

N. EL Mekkaoui, S. Idrissi, S. Mtougui, I. EL Housni, R. Khalladi, S. Ziti, H. Labrim, L. Bahmad

Chin. Phys. B . 2019, 28(9): 097503 . **doi:** 10.1088/1674-1056/ab3441

Temperature-dependent interlayer exchange coupling strength in synthetic antiferromagnetic$[Pt/Co]_2/Ru/[Co/Pt]_4$ multilayers

Yong Li(李勇), Xiangjun Jin(金香君), Pengfei Pan(潘鹏飞), Fu Nan Tan, Wen Siang Lew, Fusheng Ma(马付胜)

Chin. Phys. B . 2018, 27(12): 127502 . **doi:** 10.1088/1674-1056/27/12/127502

Fabrication and magnetic properties of $4SC(NH_2)_2$-$Ni_{0.97}Cu_{0.03}Cl_2$ single crystals

Chen Li-Min, Guo Ying, Liu Xu-Guang, Xie Qi-Yun, Tao Zhi-Kuo, Chen Jing, Zhou Ling-Ling, Liu Chun-Sheng

Chin. Phys. B . 2015, 24(12): 127503 . **doi:** 10.1088/1674-1056/24/12/127503

Antiferromagnetic and topological states in silicene: A mean field study

Liu Feng, Liu Cheng-Cheng, Yao Yu-Gui

Chin. Phys. B . 2015, 24(8): 087503 . **doi:** 10.1088/1674-1056/24/8/087503

Model of hybrid interfacial domain wall in ferromagnetic/antiferromagnetic bilayers

Zhang Wen, Zhai Ya, Lu Mu, You Biao, Zhai Hong-Ru, Caroline G Morgan

Chin. Phys. B . 2015, 24(4): 047502 . **doi:** 10.1088/1674-1056/24/4/047502

Metamagnetic transition and reversible magnetocaloric effect in antiferromagnetic DyNiGa compound*

Yan-Hong Ding(丁燕红)[1,†], Fan-Zhen Meng(孟凡振)[1], Li-Chen Wang(王利晨)[2,3,4,‡], Ruo-Shui Liu(刘若水)[3], and Jun Shen(沈俊)[2,4]

[1] *School of Electrical and Electronic Engineering, Tianjin Key Laboratory of Film Electronic and Communication Devices, Tianjin University of Technology, Tianjin* 300384, *China*

[2] *Key Laboratory of Cryogenics, Technical Institute of Physics and Chemistry, Chinese Academy of Sciences, Beijing* 100190, *China*

[3] *Department of Physics, Capital Normal University, Beijing* 100048, *China*

[4] *University of Chinese Academy of Sciences, Beijing* 100049, *China*

(Received 11 February 2020; revised manuscript received 20 April 2020; accepted manuscript online 7 May 2020)

Rare-earth (*R*)-based materials with large reversible magnetocaloric effect (MCE) are attracting much attention as the promising candidates for low temperature magnetic refrigeration. In the present work, the magnetic properties and MCE of DyNiGa compound with TiNiSi-type orthorhombic structure are studied systematically. The DyNiGa undergoes a magnetic transition from antiferromagnetic (AFM) to paramagnetic state with Néel temperature $T_N = 17$ K. Meanwhile, it does not show thermal and magnetic hysteresis, revealing the perfect thermal and magnetic reversibility. Moreover, the AFM state can be induced into a ferromagnetic state by a relatively low field, and thus leading to a large reversible MCE, *e.g.*, a maximum magnetic entropy change ($-\Delta S_M$) of 10 J/kg·K is obtained at 18 K under a magnetic field change of 5 T. Consequently, the large MCE without thermal or magnetic hysteresis makes the DyNiGa a competitive candidate for magnetic refrigeration of hydrogen liquefaction.

Keywords: DyNiGa, antiferromagnetic, magnetocaloric effect, first-order phase transition

PACS: 75.30.Sg, 75.50.Bb, 75.60.Ej **DOI:** 10.1088/1674-1056/ab90f3

1. Introduction

In recent years, magnetic refrigeration based on magnetocaloric effect (MCE) has emerged as a green cooling technology, which shows a promising future due to its advantages of energy conservation and environmental protection in comparison with the traditional gas compression refrigeration. The MCE is one of the fundamental thermodynamic effects of magnetic materials, which can induce temperature change by exposing the MCE material to a changing magnetic field.[1–6] The magnitude of MCE is generally characterized by the adiabatic temperature change (ΔT_{ad}) and/or the isothermal magnetic entropy change (ΔS_M) under the change of magnetic field.[7–9] According to their working temperature ranges, magnetocaloric materials are usually divided into low temperature zone (below 20 K), medium temperature zone (20 K–77 K), and high temperature zone (77 K–300 K).[5] The materials working at high temperature especially around room temperature show their potential applications in air conditioners and storage cabinets. On the other hand, the magnetic refrigeration materials at medium and low temperatures are also important for the high demands of gas liquefaction and scientific research. Therefore, much attention has been paid to the search for low temperature magnetic materials with large MCE.

Although the paramagnetic salts, such as $Gd_3Ga_5O_{12}$, $GdLiF_4$, and GdF_3, have been successfully used to obtain ultra-low temperature, their MCEs decrease remarkably with temperature increasing, which limits their application. What is worse is that the thermal conductivity of paramagnetic salts is relatively low, and so it is very disadvantageous for their working in magnetic refrigeration. In contrast, recently rare-earth (*R*)-based materials have been found to exhibit larger MCEs, higher thermal conductivities, and less temperature dependence, thus becoming the promising candidates for low temperature magnetic refrigeration.

As one of the typical *R*-based material families, the *RTX* (R = rare earth, T = transitional metal, X = main group element) ternary intermetallics have been studied widely due to their high MCE at low temperatures.[10–13] In addition to the large MCE reported in ferromagnetic (FM) *RTX* compounds, such as *R*FeSi[14,15] and *R*CoAl,[10,16] it is interesting to find that some antiferromagnetic (AFM) *RTX* compounds, such as *R*NiSi[17] and *R*CuSi,[12,18] also show high MCEs due to the field-induced metamagnetic transition from AFM to FM

*Project supported by the National Natural Science Foundation of China (Grant Nos. 51701130 and 51925605), the Natural Science Foundation of Tianjin, China (Grant Nos. 18ZXCLGX00040 and 15JCZDJC38700), and the National Key Research and Development Program of China (Grant Nos. 2019YFA0704900, 2019YFA0705000, 2019YFA0705100, 2019YFA0705200, and 2019YFA0705300).

†Corresponding author. E-mail: lucydyh@163.com

‡Corresponding author. E-mail: wanglichen@mail.ipc.ac.cn

© 2020 Chinese Physical Society and IOP Publishing Ltd

states. Meanwhile, it is found that no hysteresis loss appears during the first-order AFM–FM metamagnetic transition, and so this excellent magnetic reversibility is desirable for the magnetic refrigeration cycle.[13] These results expand the research scope of MCE materials, and also impel people to search for novel AFM materials with large MCE.

In previous studies, Canepa *et al.* reported that the GdNiGa exhibits FM ground state and shows a large MCE around the $T_C = 30.5$ K.[19] On the contrary, the HoNiGa has been found to behave an AFM ground state, and then presents a large reversible MCE induced by metamagnetic transition.[13] In order to study its magnetic and magnetocaloric properties varying with the change of *R* element, we further study the magnetic properties and MCE of DyNiGa systematically in the present work.

2. Materials and experiments

The elements Dy, Ni, and Ga each with a purity of 99.9 wt% were chemically weighed after the oxide layer on the surface had been polished. Then, the starting materials were melted in a tungsten non-consumable electric arc furnace with high purity argon gas protection. In order to obtain a single phase DyNiGa compound, the sample was melted five times and then annealed at 850 ℃ for 1 week. Before being annealed, the obtained sample was sealed in a quartz tube filled with high-purity argon gas. The crystal structure and phase of the sample were examined by x-ray diffractometer (D8, Bruker) through using a Cu target and refined by using the LHPM Rietica software. The magnetic properties were measured by SQUID-VSM superconducting quantum magnetometer (SQUID, Quantum Design).

3. Results and discussion

Figure 1 shows the experimental and refined powder XRD patterns of DyNiGa compound at room temperature. The Rietveld refinement based on the XRD pattern reveals that the DyNiGa crystallizes into a pure TiNiSi-type orthorhombic structure (space group *Pnma*), and no impurity phase can be found in the DyNiGa compound. The lattice parameters *a*, *b*, *c*, and unit cell volume are determined to be $a = 6.8520(4)$ Å, $b = 4.2834(3)$ Å, $c = 7.3438(4)$ Å, and cell volume = 215.54(2) Å^3, respectively, which are consistent with the earlier reported results.[20] It is noted that the lattice parameters of DyNiGa are smaller than those of GdNiGa but larger than the ones of HoNiGa,[13,19] and this result is attributed to the lanthanide contraction.

Figure 2 displays the curves of magnetization *versus* temperature (*M*–*T*) of the DyNiGa compound under 0.01 T in the zero-field cooling (ZFC) and field-cooling (FC) processe, respectively. A λ-type peak around 17 K appears separately in both ZFC and FC curves, indicating that the DyNiGa undergoes a typical AFM–PM transition around the Néel temperature $T_N = 17$ K. Meanwhile, it is noted that the magnetization does not approach to zero even at 150 K. Considering the fact that no impurity phase has been identified by XRD study, this result implies the possible presence of short-range magnetic correlation above T_N.[21] In addition, the ZFC and FC curves overlap with each other perfectly, suggesting the absence of thermal hysteresis. This fact is desirable for the applications of this material in magnetic refrigeration.

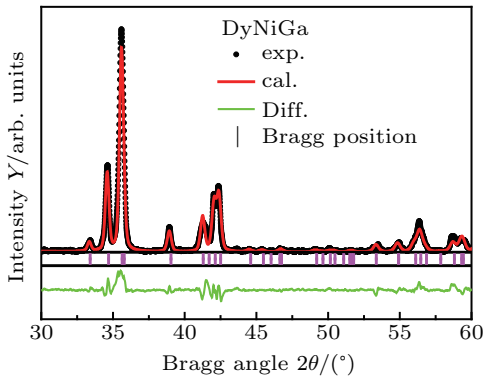


Fig. 1. Powder XRD patterns of DyNiGa compound at room temperature.

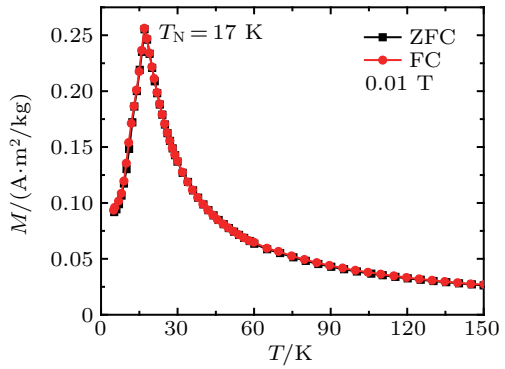


Fig. 2. Temperature-dependent magnetizations under 0.01 T measured in ZFC and FC modes for DyNiGa compound.

The inverse DC susceptibility ($1/\chi$) is derived from the ZFC *M*–*T* curve under a low field of 0.01 T, and then the temperature dependence of $1/\chi$ fitted to the Curie–Weiss law $\chi^{-1} = (T - \theta_p)/C_m$ (C_m is the Curie–Weiss constant) is plotted in Fig. 3. The paramagnetic Curie temperature (θ_p) and effective magnetic moment (μ_{eff}) can be obtained by the Curie–Weiss fit based on the $1/\chi$–*T* curve. It is clearly seen that the $1/\chi$ matches well with the Curie–Weiss law in the paramagnetic region far above T_N. The μ_{eff} value is determined to be 10.00 μ_B, which is slightly lower than the theoretical magnetic moment of Dy^{3+} free ion (10.63 μ_B). This lower μ_{eff} is probably attributed to crystalline electric field (CEF) effect, which causes it to slightly deviate from the Curie–Weiss behavior at low temperatures.[22,23] In addition, the θ_p value is obtained to be −12.5 K by extrapolating the fitting line to $1/\chi = 0$ as indicated in Fig. 3. As is well known, the θ_p value represents the

sum of all magnetic interactions in magnetic materials, and the AFM material will exhibit a negative θ_p value while the FM material shows a positive θ_p. Thus, the negative θ_p of DyNiGa under 0.01 T further confirms the AFM ground state of DyNiGa compound.

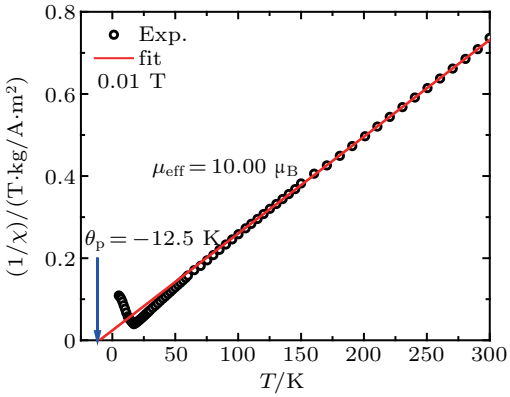


Fig. 3. Variation of inverse dc susceptibility with temperature under 0.01 T fitted to the Curie–Weiss law.

Figure 4 displays the isothermal magnetization curves (a) below T_N and (b) above T_N with magnetic fields going up to 5 T. It can be obviously seen from Fig. 4(a) that the magnetization at 5 K first increases slowly with magnetic field increasing, and then sharply increases around a critical magnetic field ($\mu_0 H_{cr}$) of 0.6 T, indicating the occurrence of field-induced metamagnetic transition from AFM to FM states. Below the $\mu_0 H_{cr}$, the magnetization increases with temperature increasing, which is corresponding to the characteristic of AFM state, while it decreases with the increase of temperature above the $\mu_0 H_{cr}$, indicating the behavior of FM state. This $\mu_0 H_{cr}$ is larger than that (0.5 T at 2 K) of HoNiGa, suggesting that the AFM exchange interaction of DyNiGa is stronger than that of HoNiGa.[13] Figure 4(b) shows that the magnetization decreases gradually with temperature further increasing above T_N, which corresponds to the PM state induced by the thermal disturbance. Meanwhile, it is also found that the M–H curves still show obvious curvatures at temperatures far above T_N. This result further proves that the short-range magnetic correlations appears above T_N. Moreover, the M–H curves are measured in the magnetic field increasing and decreasing mode in order to study the magnetic reversibility of DyNiGa, and magnetic hysteresis is found in none of these magnetization isotherms. As is well known, the thermal and magnetic hysteresis will reduce the efficiency of magnetic refrigeration through the hysteresis loss.[5,24] Therefore, the absence of thermal nor magnetic hysteresis is highly favorable to the magnetic refrigeration cycle.

Figure 5 presents the Arrott-plots (M^2 *versus* H/M) for DyNiGa compound (a) below T_N and (b) above T_N, respectively. According to the Banerjee criterion, the magnetic transition is considered to be of first-order nature if the Arrott plot shows a negative slope or an inflection point, while it is of second-order nature when the Arrott plot exhibits positive slope.[25] The Arrott plots below T_N show distinct negative slopes as shown in Fig. 5(a), and thus confirming the nature of the first-order field-induced metamagnetic transition from AFM to FM state. In contrast, figure 5(b) shows that the Arrott plots present positive slopes above T_N, suggesting the second-order field-induced PM–FM transition.

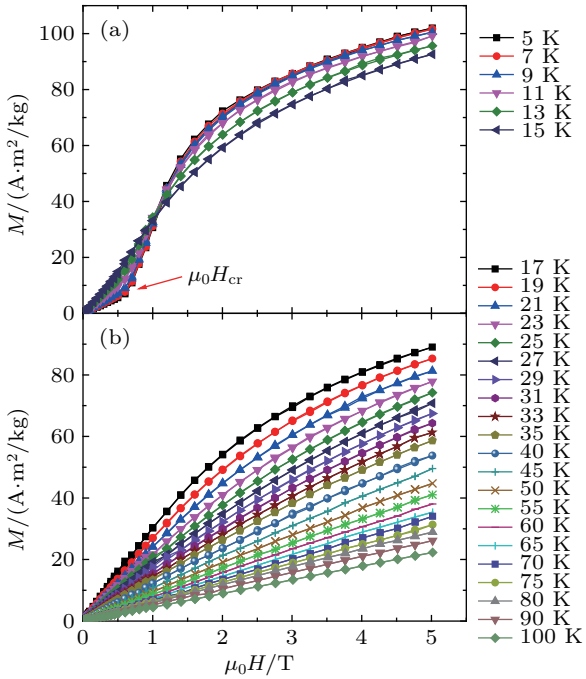


Fig. 4. M–H curves of DyNiGa compound (a) below and (b) above T_N with magnetic fields increasing from 0 to 5 T for various temperatures.

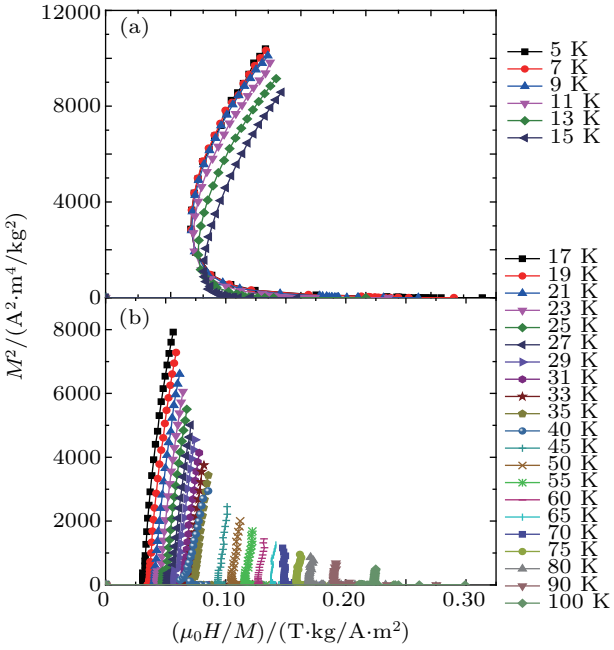


Fig. 5. Arrott-plots of DyNiGa (a) below and (b) above T_N in field increasing process for various temperatures.

The isothermal magnetic entropy change ΔS_M can be estimated based on the isothermal magnetization data by using

Maxwell's relationship

$$\Delta S_{\mathrm{M}} = \int_0^H (\partial M/\partial T)_H \mathrm{d}H. \quad (1)$$

The plots of ΔS_{M} of DyNiGa *versus* temperature (ΔS_{M}–T) for different magnetic field changes are shown in Fig. 6. The positive values of ΔS_{M}, so called "inverse MCE", are found to change below T_{N} under low magnetic field. This phenomenon corresponds to the AFM ground state of DyNiGa. With magnetic field increasing higher than 1 T, the sign of ΔS_{M} changes from positive to negative, which is due to the field-induced AFM–FM metamagnetic transition. For a magnetic field change of 5 T, a maximum $-\Delta S_{\mathrm{M}}$ value of 10 J/kg·K can be obtained at 18 K, very close to the liquid hydrogen temperature (20.3 K).[14] This relatively large MCE is attributed to the field-induced AFM–FM metamagnetic transition, which results in the enhanced magnetization and large variation of magnetization with temperature. The $-\Delta S_{\mathrm{M}}$ value of DyNiGa is comparable to those of other top-quality MCE materials, such as DyCuAl, *R*Si, and RNi_5 in a similar temperature range.[26–28] Therefore, the large MCE without thermal or magnetic hysteresis suggests that DyNiGa can be potential candidate for the low temperature magnetic refrigeration of hydrogen liquefaction.

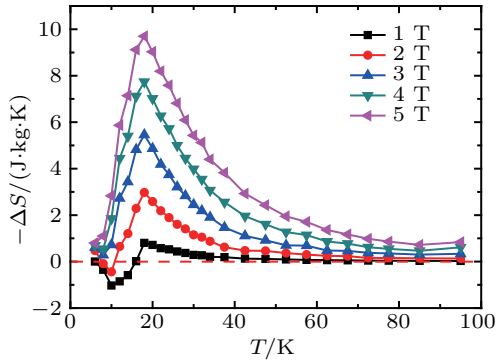


Fig. 6. Plots of magnetic entropy *versus* temperature for DyNiGa compound under various magnetic field changes and different temperatures.

4. Conclusions

In this work, the DyNiGa compound with TiNiSi-type orthorhombic structure is prepared, and its magnetic properties and magnetocaloric effect are studied systematically. The DyNiGa compound experiences an AFM-to-PM transition at $T_{\mathrm{N}} = 17$ K. Neither thermal hysterisis nor magnetic hysteresis is observed, indicating the perfect thermal and magnetic reversibility existing. Moreover, the AFM state can be tranformed into FM state by a relatively low field, and then leading to a large $-\Delta S_{\mathrm{M}}$ of 10 J/kg·K around 18 K for a magnetic field change of 5 T. Therefore, large magnetocaloric effect with no hysteresis loss suggests that DyNiGa can be a promising candidate of magnetic refrigeration material for magnetic refrigeration of hydrogen liquefaction.

References

[1] Franco V, Blázquez J S and Conde A 2006 *Appl. Phys. Lett.* **89** 222512
[2] Pecharsky V K and Gschneidner Jr K A 1997 *Phys. Rev. Lett.* **78** 4494
[3] Hu F X, Shen B G, Sun J R and Zhang X X 2000 *Chin. Phys.* **9** 550
[4] Tegus O, Brück E, Buschow K H J and de Boer F R 2002 *Nature* **415** 150
[5] Zheng X Q, Shen J, Hu F X Sun J R and Shen B G 2016 *Acta Phys. Sin.* **65** 217502 (in Chinese)
[6] Barclay J A and Steyert W A 1982 *Cryogenics* **22** 73
[7] Wada H and Tanabe Y 2001 *Appl. Phys. Lett.* **79** 3302
[8] Wang Y X, Zhang H, Liu E K, Zhong X C, Tao K, Wu M L, Xing C F, Xiao Y N, Liu J and Long Y 2018 *Adv. Electron. Mater.* **4** 1700636
[9] Zheng X Q, Xu J W, Zhang H, Zhang J Y, Wang S G, Zhang Y, Xu Z Y, Wang L C and Shen B G 2018 *AIP Adv.* **8** 056432
[10] Zhang H, Shen B G 2015 *Chin. Phys. B* **24** 127504
[11] Gupta S and Suresh K G 2015 *J. Alloys Compd.* **618** 562
[12] Chen J, Shen B G, Dong Q Y, Hu F X, Sun J R 2010 *Appl. Phys. Lett.* **96** 152501
[13] Wang Y X, Zhang H, Wu M L, Tao K, Li Y W, Yan T, Long K W, Long T, Pang Z and Long Y 2016 *Chin. Phys. B* **25** 127104
[14] Zhang H, Shen B G, Xu Z Y, Shen J, Hu F X, Sun J R and Long Y 2013 *Appl. Phys. Lett.* **102** 092401
[15] Zhang H, Sun Y J, Niu E, Yang L H, Shen J, Hu F X, Sun J R and Shen B G 2013 *Appl. Phys. Lett.* **103** 202412
[16] Zhang X X, Wang F W and Wen G H 2001 *J. Phys.: Condes. Matter* **13** L747
[17] Zhang H, Wu Y Y, Long Y, Wang H S, Zhong K X, Hu F X, Sun J R and Shen B G 2014 *J. Appl. Phys.* **116** 213902
[18] Chen J, Shen B G, Dong Q Y and Sun J R 2010 *Solid State Commun.* **150** 1429
[19] Canepa F, Napoletano M, Palenzona A, Merlo F and Cirafici S 1999 *J. Phys. D: Appl. Phys.* **32** 2721
[20] Vasilechko L O and Grin Y 1996 *Inorg. Mater.* **32** 512
[21] Arora P, Chattopadhyay M K, Chandra L S S, Sharma V K and Roy S B 2011 *J. Phys.: Condes. Matter* **23** 056002
[22] Mo Z J, Shen J, Yan L Q, Wu J F, Wang L C, Lin J, Tang C C and Shen B G 2013 *Appl. Phys. Lett.* **102** 192407
[23] Gupta S, Rawat R and Suresh K G 2014 *Appl. Phys. Lett.* **105** 012403
[24] Zheng X Q and Shen B G 2017 *Chin. Phys. B* **26** 027501
[25] Banerjee S K 1964 *Phys. Lett.* **12** 16
[26] Liu R S, Liu J, Wang L C, Li Z R, Yu X, Mi Y, Dong Q Y, Li K, Li D L, Lv C H, Liu L F and He S L 2020 *Chin. Phys. Lett.* **37** 017501
[27] Dong Q Y, Shen B G, Chen J, Shen J, Zhang H W and Sun J R 2009 *J. Appl. Phys.* **105** 113902
[28] von Ranke P J, Mota M A, Grangeia D F, Magnus A, Carvalho G, Gandra F C G, Coelho A A, Caldas A, de Oliveira N A and Gama S 2004 *Phys. Rev. B* **70** 134428